Heliyon 9 (2023) e16788

Contents lists available at ScienceDirect

Heliyon

journal homepage: www.cell.com/heliyon

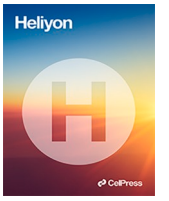

Research article

Evaluation of AGM and FEM method for thermal radiation on nanofluid flow between two tubes in nearness of magnetism field

As'ad Alizadeh [a,**], Seyedeh Fatemeh Shahabi Takami [b], Reza Iranmanesh [c], Pooya Pasha [d,*]

[a] Department of Civil Engineering, College of Engineering, Cihan University-Erbil, Erbil, Iraq
[b] Department of Mathematics, Pure Mathematic, Analytical Tendency, Iran University of Science and Technology Narmak, 16846, Tehran, Iran
[c] Faculty of Civil Engineering, K.N. Toosi University of Technology, Tehran, 158754416, Iran
[d] Department of Mechanical Engineering Mazandaran University of Science and Technology, Babol, Iran

ARTICLE INFO

Keywords:
Thermal radiation
Nanofluid
Magnetism amplitude
AGM and FEM

ABSTRACT

The nanofluid flow through two orbicular cylinders is explored utilizing the overall Koo–Kleinstreuer–Li (KKL) model within the nearness of a magnetic field. The impact of thermal radiation is considered in the energy equation. The novelty of this study is examining convective heat transfer for nanofluid flow between two flat tubes with the Akbari-Ganji method and Finite Element Techniques to examine the heat flux field by implies of 2D forms of temperature and velocity at unprecedented Reynolds numbers. The approaches for solving ODEs are AGM and FEM. Semi-analytical methods are assessed for specific parameters of aspect ratio, Hartmann number, Eckert number, and Reynolds quantity with various values. Adding *Ha*, Ec, and G causes the temperature gradient to grow, while adding the Reynolds number causes it to decrease. As the Lorentz forces increase, the velocity decreases; nevertheless, as the Reynolds number rises, the velocity decreases. With the reduction of the fluid's dynamic viscosity, the temperature will decrease, which will decrease the thermal trend along the vertical length of the pipes.

1. Introduction

Magnetic hydrodynamic convective free flow has wide applications in industries, mechanics, and bioscience. Especially in the last decade, nanotechnology has been displayed as a better approach to improving heat conveyance. The principle of magnetohydrodynamics (MHD) is a critical interdisciplinary field. One of the essential applications of this effect is pumping materials that are difficult to pump with conventional pumps. Among the actual examples of this model, we can refer to this sentence: Various renewable energy systems such as solar energy, waste heat recovery, geothermal energy, combustion, latent heat storage, and air conditioning. MHD material science is concerned with the impacts of the magnetism field on the energetic conducting liquid. The vital of the MHD control era is based on Faraday's law of electromagnetic acceptance, which states that when a conductor and a magnetic field move relative to each other, at that point, the voltage is initiated within the conductor [1–8]. Salehi et al. [9] examined the hydrothermal investigation of Magneto hydrodynamic squeezing mix liquid suspended via hybrid nanoparticles. This paper examines the cross-breed nanoparticle, whereas Particles are Fe3O4 and Mos2. Akbari has fathomed the nonlinear conditions- Ganji's method and the numerical

* Corresponding author.
** asad.alizadeh2010@gmail.com
E-mail addresses: asad.alizadeh2010@gmail.com (A. Alizadeh), poooyaenginer@gmail.com (P. Pasha).

https://doi.org/10.1016/j.heliyon.2023.e16788
Received 7 November 2022; Received in revised form 17 May 2023; Accepted 18 May 2023
Available online 30 May 2023

Nomenclature

Cp	Specific heat (kJ/kg.K)
Ec	Eckert number)dimensionless number(
u	Dimensionless velocity (m/s)
B	Stable applied magnetic amplitude
Pr	Prandtl number)dimensionless number(
Ha	Hartmann number)dimensionless)
Nu	Nusselt number)dimensionless number(
Re	Reynolds number)dimensionless)
Rd	Radiation (dimensionless)
T	Temperature (K)
k	Thermal conductivity ($Wm^{-1}K^{-1}$)
ω	Stable circulation velocity (rad/s)
θ	Dimensionless
α	Thermic diffusivity (m2/s)
μ	Dynamic viscosity (Pa.s)
φ	Capacity fraction (%)
ρ	Density (kg/m3)

strategy compare the result. Ghadikolaei et al. [10] studied the Magneto hydro dynamic boundary layer examination to place micropolar dusty liquid containing hybrid nanoparticles over a porous environment. The temperature has also increased due to the Hartman number update since the Joule heating influence, according to the results of his study. The range of temperature and velocity in the x-course and the precise velocity at which nanofluids flow through triangular, chamfer, and rectangular blades, were investigated by Shadman et al. The effect of the magnetic field on the displacement of energy has been reported by Sheikhul-Islami and colleagues [11]. The results of their research stated that the higher cap velocity, including the impact of Kelvin s strengths, is more noticeable. Bondarova et al. [12] used Buongiorno's math design for the effect of magnetic energy on absolute temporal convection. Sheikh al-Islami and Rukni [13] investigated the impact of Lorentz strengths on absolute convection in a moiety. Bondarova et al.'s [14] headline analysis was used to simulate MHD absolute convection in a full-blown depth. Sheikhul-Islami and Vajrawallu [15] examined nanofluid flow and heat transfer in-depth with uncertain Lorentz strengths. Shermet et al. [16] analyzed the magnetism amplitude on absolute convection. Their wavy light depth displayed a corner radiator impact on nanofluid ooze. Semi-analytic strategies can illuminate nonlinear conditions. There are a few semi-analytic strategies, such as DTM [17–19], HPM [20,21], HAM [22], ADM [23,24], OHAM [25,26], etc. One of the foremost later and influential semi-analytic come closes is AGM. Mirgol Babaei et al. [27] utilized the Akbari-Ganji strategy so that Duffing is not a linear oscillator. They demonstrated the realness of this issue. Nanofluid efflux and heat transfer have been reenacted by a few creators within the final decade [28–30]. Ferdosi and his colleagues [31] researched the changes in buckling systems in various types of carbon tubes. Moradi and his colleagues [32] conducted extensive studies on improving heat transfer and oil pressure drop in a nanofluid's hydraulic and thermal systems. Asgari and his colleagues [33] conducted various research on increasing the heat transfer properties of carbon nanotubes through nitrogen doping. The results appeared to be a 32.7% enhancement in convective heat transfer coefficient at a Reynolds number of 8676 and a 27% increment in thermal conductivity at 0.5 mass% and 30 °C. Nanoparticles are used in various fields, such as solar collectors, petrochemicals, and chemical engineering, due to their superior properties to conventional fluids [34]. Also, researchers conducted many studies regarding the effects of magnetic parameters and solar energy on fluids and nanofluids passing through flat plates. The amount of radiation was also calculated while calculating the impact of the parameters of the Prandtl number and Nusselt number [35–44]. Also, researchers have conducted many studies in the field of heat flow analysis, displacement, and entropy effects around the semi-annular chamber with different nanofluids [45–48]. The primary purpose of this essay is to show the impact of magnetism purview aboard hydrothermal

Table 1(a)
The modulus measures of nanofluid.

modulus measures	Al2O3–water
a1	52.823488759
a2	6.117637295
a3	0.6958745084
a4	4.17455565786E-02
a5	0.177619300241
a6	- 298.23819084
a7	- 34.533616906
a8	- 3.9229889283
a9	- 0.2354749626
a10	- 0.999062347

operation of nanofluid betwixt two tubes. Akbari-Ganji style is utilized to fathom this issue. The designation of aspect ratio, radiation parameter, Reynolds number, Eckert number, and Hartmann number is exhibited. In addition to that, under various numerical and analytical schemes, solution time and grid generation remain significant obstacles that are easily solved by current methods, and this is a notable feature of the application of Akbari Ganji techniques. The coefficient value for Al2o3 and Thermo physical properties of water and nanoparticles, respectively, are given in Table 1& Table 2. The reasons for utilizing aluminum oxide nanofluid within the display ponder are that Compared to its equivalent nanoparticles, it includes a higher particular surface range and a high flaw of the fabric surface and specific structure of the nanoparticles. The novelty of this study is the examination of convective heat transfer for nanofluid flow between two flat tubes with AGM and FEM strategies so that we examine the heat flux field by implies of 2D forms of temperature and velocity at distinctive Reynolds numbers.

2. Governing formulae

Fig. 1 depicts the issue's geometry schematically. Laminar flow design and a two - dimensional supposition of fluid fathoming space per a consistent state are key hypotheses for this problem. The temperatures of the inner and outer tubes are maintained at constant values during expansion with the assumption that the internal tube will rotate at a constant velocity. Laminar 2D flow in cylindrical coordinates is debated (Fig. 1). The governing formulae are as below [28]:

$$\nu_{nf}\left(\frac{\partial^2 U^*}{\partial R^2}+\frac{1}{R}\frac{\partial U^*}{\partial R}-\frac{U^*}{R^2}\right)-\frac{\sigma_{nf}U^*B_0^2}{\rho_{nf}}=U^*\frac{\partial U^*}{\partial R} \tag{1}$$

$$\frac{k_{nf}}{R}\frac{\partial}{\partial R}\left(R\frac{\partial T^*}{\partial R}\right)+\mu_{nf}\left(\frac{\partial U^*}{\partial R}-\frac{U^*}{R}\right)^2-\frac{\partial q_r}{\partial R}=\left(\rho C_p\right)_{nf}U^*\frac{\partial T^*}{\partial R}$$

$$q_r=-\frac{4\sigma_e}{3\beta_R}\frac{\partial T^{*4}}{\partial R}\,.\,T^{*4}\cong 4T_2^{*3}T^*-3T_2^{*4}. \tag{2}$$

$$R=r_1:U^*(R)=\omega r_1.\,T^*=T_1^*\,.\,R=r_2:U^*(R)=0.T^*=T_2^* \tag{3}$$

ρ_{nf}, $(\rho C_p)_{nf}$, σ_{nf} Can be introduced as follows [28]:

$$\rho_{nf}=\varphi\rho_p+\rho_f(1-\varphi)$$

$$\left(\rho C_p\right)_{nf}=\varphi\left(\rho C_p\right)_p+\left(\rho C_p\right)_f(1-\varphi) \tag{4}$$

$$\frac{\sigma_{nf}}{\sigma_f}=1+\frac{3\left(\sigma_p/\sigma_f-1\right)\varphi}{\left(\sigma_p/\sigma_f+2\right)-\left(\sigma_p/\sigma_f-1\right)\varphi}$$

k_{nf} Is gotten matching Koo–Kleinstreuer–Li (KKL) model [28]:

$$k_{nf}=k_f\left(\frac{3\left(k_p/k_f-1\right)\varphi}{-\left(k_p/k_f-1\right)\varphi+\left(k_p/k_f+2\right)}+1\right)+5\varphi\times10^4C_{pf}g'\left(d_p\,.\,T^*\,.\,\varphi\right)\rho_f\sqrt{\frac{k_bT^*}{\rho_pd_p}} \tag{5}$$

$$g'\left(d_p,T^*,\varphi\right)=\left(a_1+a_2\,ln\left(d_p\right)+a_3\,ln(\varphi)+a_4\,ln\left(d_p\right)ln(\varphi)+a_5\,ln\left(d_p\right)^2\right)ln(T^*)$$
$$+\left(a_6+a_7\,ln\left(d_p\right)+a_8\,ln(\varphi)+a_9\,ln\left(d_p\right)ln(\varphi)+a_{10}\,ln\left(d_p\right)^2\right)$$

$$\mu_{nf}=\frac{\mu_f}{(1-\varphi)^{2.5}}+\frac{k_{Brownian}}{k_f}\times\frac{\mu_f}{pr} \tag{6}$$

All required factors and properties are outlined in Tables 1a and 1b [28]. The dimensionless shapes of over conditions are as takes after [28]:

$$\frac{\partial^2u(r)}{\partial r^2}+\frac{1}{r}\frac{\partial u(r)}{\partial r}-\left\{\frac{Ha^2}{(1-\eta^2)}\frac{A_5}{A_2}+\frac{1}{r^2}\right\}u(r)-Re\frac{A_1}{A_2}u(r)\frac{\partial u(r)}{\partial r}=0 \tag{7}$$

Table 1(b)
Thermal physical attributes of water and nanoparticle.

	ρ (kg/m^3)	C_P(J/gr)	K(W/m·K)	d_P (nm)	σ (P)
Pure water	997.1	4179	0.613	–	0.05
Al_2o_3	3890	880	30	5	10 E −12

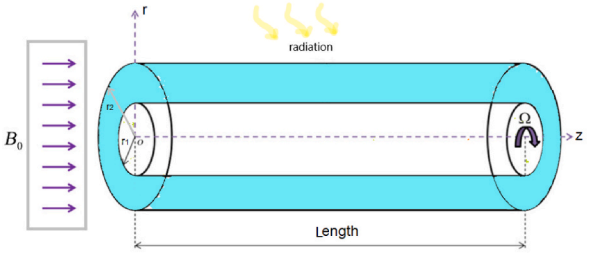

Fig. 1. Schematic of the plan under consideration.

$$\frac{\partial^2\theta(r)}{\partial r^2}+\frac{1}{r}\frac{\partial\theta(r)}{\partial r}+Ec\,Pr\frac{A_2}{A_4}\left\{\frac{\partial u(r)}{\partial r}-\frac{1}{r}u(r)\right\}^2+\frac{4Rd}{3A_4}\frac{\partial^2\theta(r)}{\partial r^2}-PrRe\frac{A_3}{A_4}u(r)\frac{\partial\theta(r)}{\partial r}=0, \tag{8}$$

$$r=\frac{R}{r_2}\ .\ u=\frac{U}{\omega r_1}\ .\ \eta=\frac{r_1}{r_2}\ .\ \theta=\frac{T-T_2}{T_1-T_2} \tag{9}$$

in the coupled equations above (obtained by the kkl method and the dimensionless operation was performed on it), u is the velocity, *Ha* is the Hartman parameter, Re is the Reynolds number, theta is the heat transfer variable, Ec is the Eckert number, Pr is the Prandtl number and Rd is the radiation variable.

The boundary conditions of the problem are considered as follows [28]:

$$r=\eta: u=1\ .\ \theta=1$$

$$r=1: u=0\ .\ \theta=0 \tag{10}$$

$$Re=\frac{\rho_f\omega r_1 r_2}{\mu_f}.Pr=\frac{\mu_f(\rho C_p)}{\rho_f k_f}.\ Ec=\frac{\rho_f(\omega r_1)^2}{(\rho C_p)_f\Delta T}.\ Rd=\frac{4\sigma_e T_c^3}{\beta_R k_f}\ .\ Ha=B_o d\sqrt{\frac{\sigma_f}{\mu_f}}$$

$$A_1=\frac{\rho_{nf}}{\rho_f}.A_2=\frac{\mu_{nf}}{\mu_f}.A_3=\frac{(\rho C_p)_{nf}}{(\rho C_p)_f}.A_4=\frac{k_{nf}}{k_f}.A_5=\frac{\sigma_{nf}}{\sigma_f} \tag{11}$$

3. A. Validation for methods

In this segment, compared AGM procedure and NUM method are used for approval. The sum of computational blunders in the AGM and WRM methods could be higher compared to the Numerical methodology in Table 2. The most extreme number of errors occurred in x = 0.5, and the least number of mistakes happened in x = 0.8.

The 2D graphs in Fig. 2 check the convergence and accuracy of the two AGM, NUM, and FEM methods concerning each other. According to Figures a-2 and c-2, with increasing distance in the r direction, first, the fluid velocity increases significantly. It reaches its highest value in the middle of the tube, but the fluid velocity decreases when passing the value of r = 0.7. We could check this process correctly using both numerical analysis methods, AGM and NUM, and the agreement between them has been established. For figures b-2 and d-2, temperature changes were checked with both techniques, and the closeness of the lines has reached its minimum, and the convergence process has progressed well.

4. Finite element method (FEM) and AGM method [29]

A finite element method (truncated as FEM) is a scalar strategy to attain a surmised solution to a course of matters administered by elliptic partial differential equations. It would be best to use mathematics to comprehensively understand and quantify physical phenomena: B. Basic or fluid behavior, heat transport, wave engendering, and living cell development. Most of these shapes are depicted by PDEs. In any case, numerical strategies have been created over the final few decades for computers to solve these PDEs, and one of the foremost prevalent nowadays is the FEM. The finite element technique can be a principal numerical procedure. One of the

Table 2
Compare results between the Akbari Ganji method, Weighted residual method [11], and NUM method for Re = 1, *Ha* = 3, Ec = 0.1, and Rd = 0.1.

	$x = 0.5$	$x = 0.6$	$x = 0.7$	$x = 0.8$	$x = 0.9$	$x = 1$
AGM	1	0.74	0.55	0.32	0.12	0
WRM	1	0.72	0.53	0.31	0.12	0
NUM	1	0. 72	0.53	0.31	0.12	0

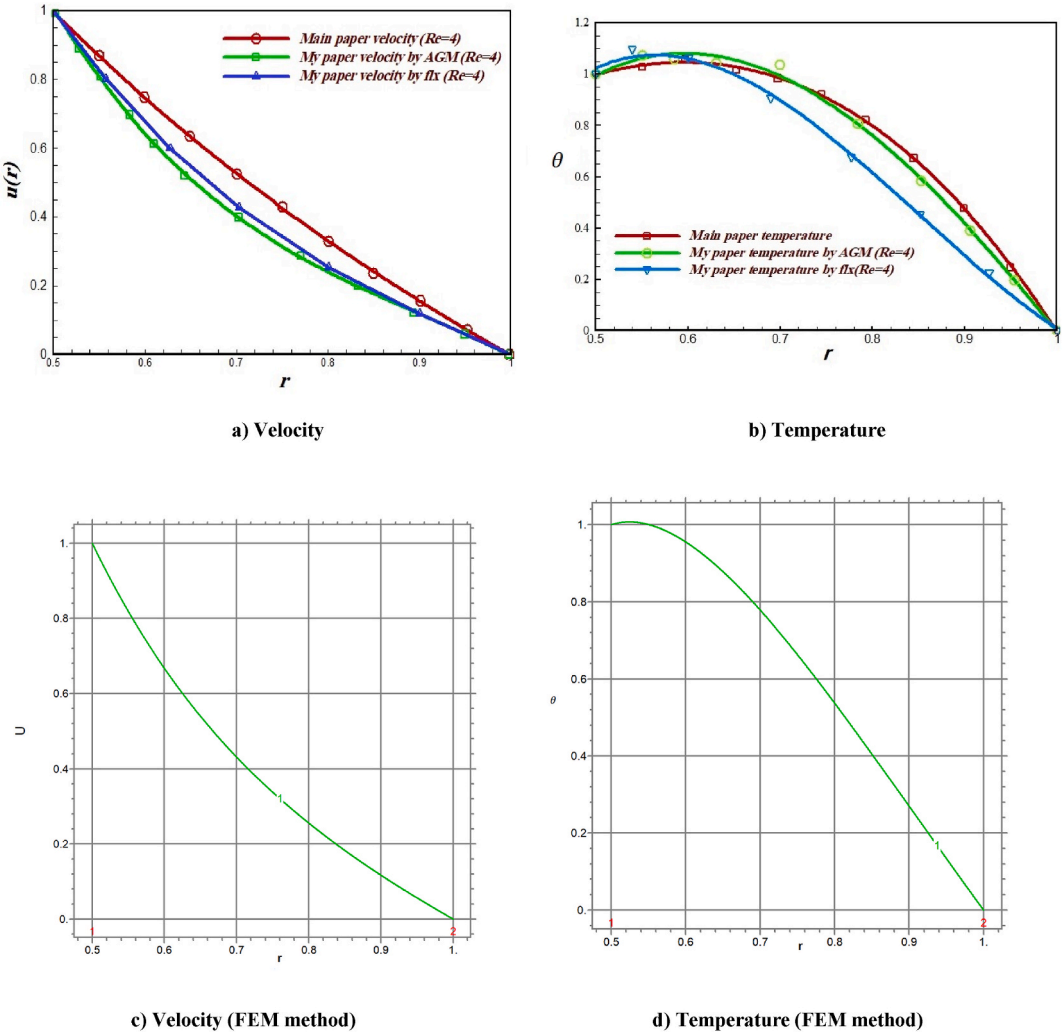

Fig. 2. Simulation of **a,c)** the velocity and **b,d)** the temperature r profile by FEM, AGM and NUM methods that solution at Re = 1, $Ha = 3$, Ec = 0.1, and Rd = 0.1.

common sense applications for this procedure is the FlexPDE program, which realizes the nonlinear fragmentary differential equations and the modulus differential equations. Interpret AGM and explain how to use it, following the description of the main equations and their boundary conditions [30]:

$$T(y) = \sum_{i=0}^{3} a_i y^i = y^3 a_3 + y^2 a_2 + y a_1 + a_0 \tag{12}$$

$$U(y) = \sum_{i=0}^{3} b_i y^i = y^3 b_3 + y^2 b_2 + y b_1 + b_0 \tag{13}$$

According to the Akbari - Ganji method, assume a test function as a solution to an equation. Perform the dissolution by adding boundary layers to the AGM equation. The boundary conditions are as follows [30]:

$$T(0) = 1 \rightarrow a_0 = 1 \tag{14}$$

$$U(0) = 1 \rightarrow b_0 = 1 \tag{15}$$

$$T(1) = 0 \rightarrow a_3 + a_2 + a_1 + a_0 = 0 \tag{16}$$

$$U(1) = 0 \rightarrow b_3 + b_2 + b_1 + b_0 = 0 \tag{17}$$

The dissolution is acquired by applying the boundary conditions to the master equation. Boundary conditions apply to the above equation. Considering the above points, we considered two test functions containing eight constant coefficients and created eight equations. The equation can be derived as follows by substituting the coefficients obtained from the described actions under the following conditions [30]:

$$T(y) = -0.16869y^3 + 0.33784y^2 - 1.16915y + 1 \tag{18}$$

$$U(y) = 0.32658y^3 - 1.02899y^2 - 0.29759y + 1 \tag{19}$$

5. The AGM method for this paper

First, let's discuss the residuals [30]:

$$F = \frac{\partial^2 u(r)}{\partial r^2} + \frac{1}{r}\frac{\partial u(r)}{\partial r} - \left\{\frac{Ha^2}{(1-\eta^2)}\frac{A_5}{A_2} + \frac{1}{r^2}\right\}u(r) - Re\frac{A_1}{A_2}u(r)\frac{\partial u(r)}{\partial r} = 0 \tag{20}$$

$$G = \frac{\partial^2 \theta(r)}{\partial r^2} + \frac{1}{r}\frac{\partial \theta(r)}{\partial r} + Ec\ Pr\frac{A_2}{A_4}\left\{\frac{\partial u(r)}{\partial r} - \frac{1}{r}u(r)\right\}^2 + \frac{4Rd}{3A_4}\frac{\partial^2 \theta(r)}{\partial r^2} - PrRe\frac{A_3}{A_4}u(r)\frac{\partial \theta(r)}{\partial r} = 0 \tag{21}$$

The arrangements of these conditions are as [30]:

$$u(r) = \sum_{i=0}^{5} a_i r^i = a_5 r^5 + a_4 r^4 + a_3 r^3 + a_2 r^2 + a_1 r + a_0, \theta(r) = \sum_{i=0}^{4} b_i r^i = b_4 r^4 + b_3 r^3 + b_2 r^2 + b_1 r + b_0 \tag{22}$$

We regard a test work as the equation's arrangement in agreement with AGM [30]:

$$r = \eta : u = 1\ .\ \theta = 1 \tag{23}$$

$$r = 1 : u = 0\ .\ \theta = 0 \tag{24}$$

Agreeing to underneath conditions, all consistent parameters can be obtained [30]:

$$u(r) = u(B.C), \theta(r) = \theta(B.C)$$

$$F(B.C) = O, G(B.C) = O \tag{25}$$

$$F'(B.C) = 0, G'(B.C) = O$$

$$\mathrm{u}(0.5) = 1 \rightarrow\ 0.3125\mathrm{e} - 1.\mathrm{a}_5 + 0.625\mathrm{e} - 1.\mathrm{a}_4 + 0.125.\mathrm{a}_3 + 0.25.\mathrm{a}_2 + 0.5.\mathrm{a}_1 + \mathrm{a}_0 = 1 \tag{26}$$

$$\mathrm{u}(1) = 0 \rightarrow\ \mathrm{a}_5 + \mathrm{a}_4 + \mathrm{a}_3 + \mathrm{a}_2 + \mathrm{a}_1 + \mathrm{a}_0 = 0 \tag{27}$$

$$\theta(0.5) = 1 \rightarrow 0.625\mathrm{e} - 1.\mathrm{b}_4 + 0.125.\mathrm{b}_3 + 0.25.\mathrm{b}_2 + 0.5.\mathrm{b}_1 + \mathrm{b}_0 = 1 \tag{28}$$

$$\theta(1) = 0 \rightarrow \mathrm{b}_4 + \mathrm{b}_3 + \mathrm{b}_2 + \mathrm{b}_1 + \mathrm{b}_0 = 0 \tag{29}$$

Applying the boundary equation to the primary equation yields the answer. The equation mentioned above is subjected to the boundary conditions. Given the abovementioned facts, we considered 2 test functions with five constant coefficients and eight equations [30]:

$$\begin{aligned}\{&\mathrm{a}_0 = -0.9706372496\mathrm{e} - 1 + 0.2904894223, \mathrm{a}_1 = 11.61708802 + .8346881589.\mathrm{I}, \mathrm{a}_2 = -34.42044012 - 3.954228212.\mathrm{I},\\ &\mathrm{a}_3 = 42.61962734 - 0.3246490943\mathrm{e} - 1.\mathrm{I}, \mathrm{a}_4 = -26.16314603 + 6.251497737.\mathrm{I}, \mathrm{a}_5 = 6.443934516 - 3.389982197.\mathrm{I},\\ &\mathrm{b}_0 = -0.8259722863 - 2.518520916.\mathrm{I}, \mathrm{b}_1 = 10.11650894 + 13.05735075.\mathrm{I}, \mathrm{b}_2 = -17.84658165 - 24.13641918.\mathrm{I},\\ &\mathrm{b}_3 = 11.11376669 + 18.78561605.\mathrm{I}, \mathrm{b}_4 = -2.557721688 - 5.188026704.\mathrm{I}\}\end{aligned} \tag{30}$$

For example, under the following conditions, by substituting the coefficients obtained from the actions explained, one can derive equations like the following [30]:

$$\mathrm{U(r)} = 5.125670753.\mathrm{r}^5 - 20.03056984.\mathrm{r}^4 + 31.68800953.\mathrm{r}^3 - 25.20682071.\mathrm{r}^2 + 7.982545767.\mathrm{r} + .44116450 \tag{31}$$

$$\theta(\mathrm{r}) = -0.5541266969.\mathrm{r}^4 + 5.633392669.\mathrm{r}^3 - 13.61422916.\mathrm{r}^2 + 9.601894124.\mathrm{r}^{-1}.066930937 \tag{32}$$

6. Results and discussion

The flow of Al_2o_3 water nanoparticles in a loop is examined logically utilizing the Akbari-Ganji technique and FEM technique. The efficacies of horizontal magnetic amplitude and heat radiation are considered. The effects of the effective parameters are shown in a

diagram. In arrange to approve the explanatory comes about, Maple 18 and FlexPDE 7, a mathematics-based computer program, are used. Evaluating shows discoveries with those taken from the Akbari - Ganji method and finite element technique solver inserted within the computer program appeared in Tables 1(b) and 2. A sensible exactitude is accomplished per consideration of mistake column sections. Fig. 3(a) shows the velocity segment as natural forces overcome viscous forces and velocity increases. As electromagnetic powers overwhelm viscose Power, velocity decrement. In this manner, the velocity increments with expanding Re but diminishes with developing *Ha*. The velocity forms for specific amounts of Hartmann numbers are displayed in Fig. 3(b). Fluid velocity decreases when electromagnetic force triumphs over sticky drive by raising the Hartmann number. As a result, a more prominent, magnetic location tends to slow the flow of fluids. Fig. 4 displays the part about temperature. It is evident that increasing Re results in larger inertia power values rather than goopy strength values, which increases the fluid velocity and raises its temperature. According to this diagram, with the fluid's dynamic viscosity reduction, the temperature will decrease, reducing the thermal trend along the vertical length of the pipes. Fig. 5(a) illustrates the range of Nusselt numbers (*Nu*) for various contents of Re at constant Hartmann numbers (*Ha*). Re has a flip-flop effect on heat transmission and *Nu*, as evidenced by the fact that when Re increases, the fluid temperature rises and, as a result, temperature angle and *Nu* number decrease. The temperature field of the fluid decreases as the radiation parameter increases, as seen in Fig. 5(b). This sentence shows that the maximum heat received from solar energy is lost on the outer surface of the tube, and as we move toward the inner tube, the heat flux decreases. Physically, the Eckert number is the ratio of the kinetic energy to the specific enthalpy difference betwixt the wall and the liquid. Therefore, as the Eckert number increases, the kinetic energy is converted into internal work energy for the stress of the viscous fluid. Fig. 5(c), the dimensionless temperature is upgraded with expanding Ec. This occurs due to the drag caused by the nanoparticles and the additional heat given through thick scattering. Fig. 6(a) shows that Rd rises as Re rises because greater Ec results in an increased viscous loss. Fig. 6(b) shows that the temperature rises as Ec rises. Figs. 5(a), 6(a) and 6(b) depict the *Nu* number changes. The Nusselt number increases as *Ha* expands, but Rd decreases as Re expands. With increased weight, the distance between the two pipes gets smaller. As a result, the aspect ratio and heat transfer rate increase

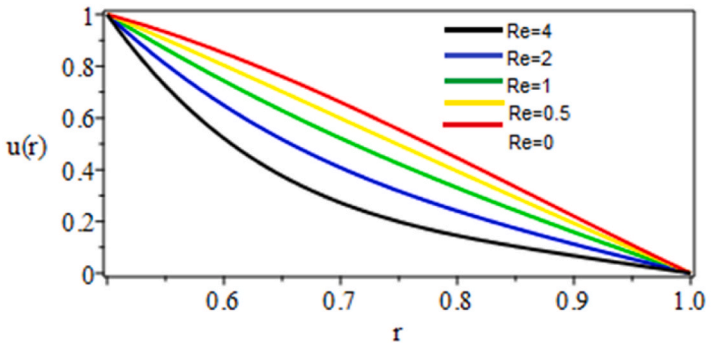

a) Effects of Reynolds parameter on velocity(Ha=3,Ec=0.1,Rd=0.1, θ =0.5, $\varphi = 0.04$,pr=6.8).

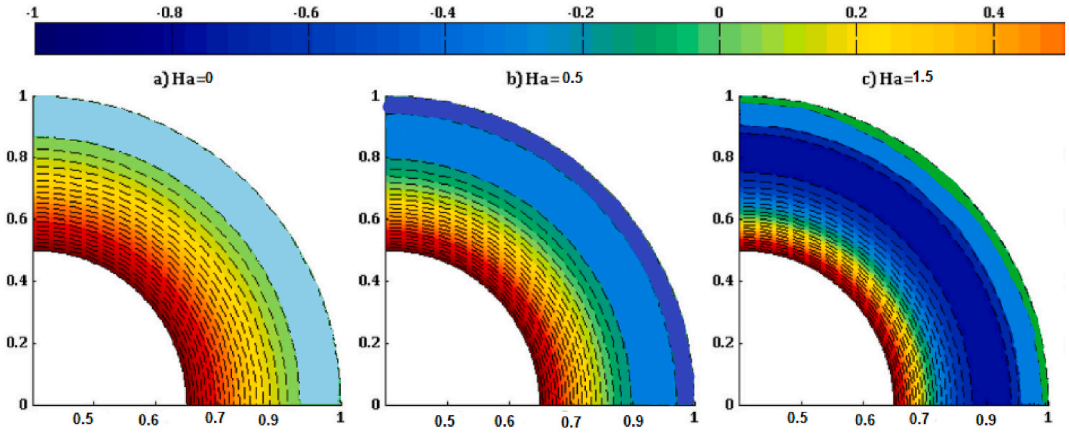

b) Velocity form for distinctive values of Hartmann number(**Ha=0, Ha=0.5, Ha=1.5**) by FEM method.

Fig. 3. Corollary for Reynolds numbers in **a)**Effects of Reynolds parameter on velocity and **b)** Velocity form for distinctive values of Hartmann number by AGM and FEM method.

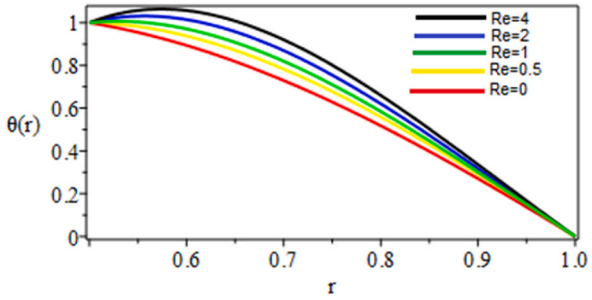

Fig. 4. Corollary for Reynolds numbers in temperature by AGM and FEM method ($Ha = 3$,Ec $= 0.1$,Rd $= 0.1$, $\theta = 0.5$, $\varphi = 0.04$,pr $= 6.8$).

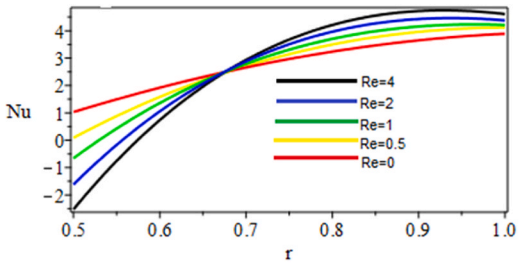

a) Changes of Nusselt number by AGM and FEM method (Ha=3,Ec=0.1,Rd=0.1, θ =0.5, φ=0.04,pr=6.8).

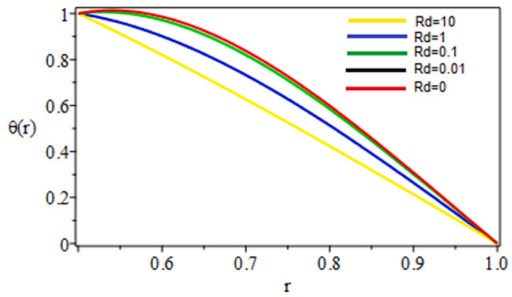

b) Changes of Rd parameter by AGM and FEM method(Ha=3,Ec=0.1,Re=0.1, θ =0.5, φ=0.04,pr=6.8).

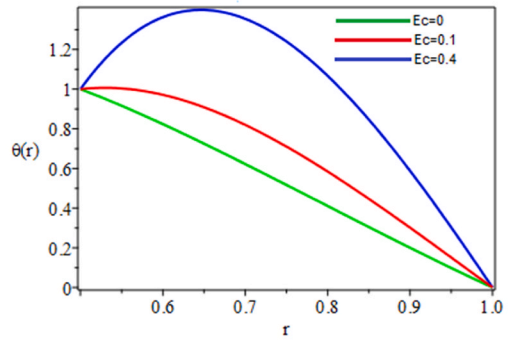

c) Changes of Ec parameter by AGM and FEM method(Ha=3,Re=0.1,Rd=0.1, θ =0.5, φ=0.04,pr=6.8).

Fig. 5. Corollary for temperature and Nusselt parameter by changes of Reynolds number(a) and Rd parameter(b) and Ec parameter(c).

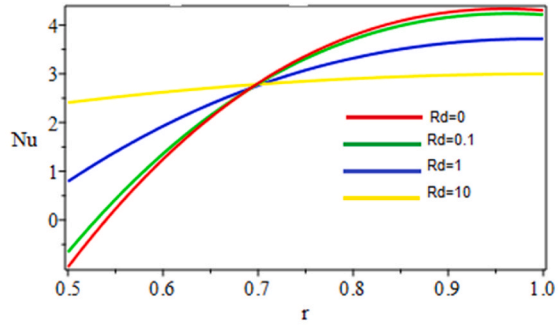

a) Changes Rd parameter by AGM and FEM method(Ha=3,Re=0.1, θ =0.5, φ=0.04,pr=6.8).

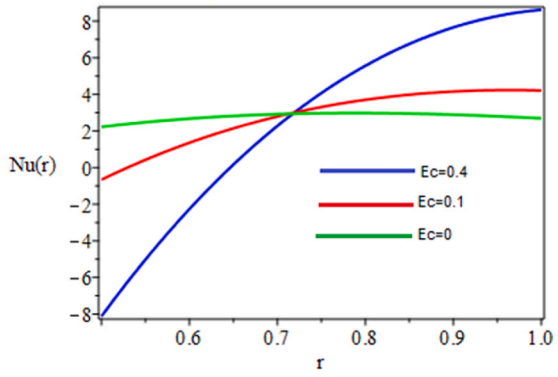

b) Changes Eckret parameter by AGM and FEM method(Ha=3,Re=0.1, θ =0.5, φ=0.04,pr=6.8).

Fig. 6. Corollary for Reynolds numbers in **a)** Rd and **b)** Ec parameter in Nusselt number by AGM and FEM method ($Ha = 3$,Re $= 0.1$, $\theta = 0.5$, $\varphi = 0.04$,pr $= 6.8$).

7. Conclusions

The nanofluid flow through two orbicular cylinders is explored utilizing the overall KKL diagram within the nearness of a magnetic field. The impact of heat radiation is considered in the energy equation. The novelty of this study is examining convective heat transfer for nanofluid flow between two flat tubes with AGM and FEM techniques to examine the heat flux field by implies of 2D forms of temperature and velocity at unprecedented Reynolds numbers. The approaches for solving ODEs are AGM and FEM. Semi-analytical methods are assessed for specific parameters of aspect ratio, Hartmann number, Eckert number, and Reynolds quantity with various values. Adding *Ha*, Ec, and G causes the temperature gradient to grow, while adding Re causes it to decrease. As the Lorentz forces increase, the velocity decreases; nevertheless, as the Reynolds number rises, the velocity decreases. Compared to Numerical methodology, the sum of computational blunders in AGM and WRM methods is low.

- The finite element strategy can be a principal numerical procedure. One of the common sense applications for this procedure is the FlexPDE program, which realizes the nonlinear fragmentary differential equations and the modulus differential equations.
- In arrange to approve the explanatory comes about, Maple 18 and FlexPDE 7; mathematics-based computer programs are utilized.
- With the reduction of the dynamic viscosity of the fluid, the temperature will decrease, which will decrease the thermal trend along the vertical length of the pipes.
- Reynolds number has a flip-flop effect on heat transmission and *Nu*, as evidenced by the fact that when Re increases, the fluid temperature rises and, as a result, temperature angle and *Nu* number decrease.

Author contribution statement

As'ad Alizadeh: Conceived and designed the analysis; Wrote the paper.
Seyedeh Fatemeh Shahabi Takami: Analyzed and interpreted the data.
Reza Iranmanesh: Contributed analysis tools or data.
Pooya Pasha: Analyzed and interpreted the data; Wrote the paper.

Funding statement
This article does not have any funding.

Data availability statement

Data will be made available on request.

Declaration of competing interest

The authors declare that they have no known competing financial interests or personal relationships that could have appeared to influence the work reported in this paper.

Acknowledgements

The authors gratefully acknowledge the support and advice of Dr. Pooya Pasha from the Department of mechanical engineering Mazandaran University of science and Technology.

References

[1] Hassan Waqas, et al., Numerical simulation for bio convection effects on MHD flow of Oldroyd-B nanofluids in a rotating frame stretching horizontally, Math. Comput. Simulat. 178 (2020) 166–182.
[2] Kh Hosseinzadeh, et al., Investigation of nano-Bioconvective fluid motile microorganism and nanoparticle flow by considering MHD and thermal radiation, Inform. Med. Unlocked 21 (2020), 100462.
[3] Muhammad Waqas, et al., Magnetohydrodynamic (MHD) mixed convection flow of micropolar liquid due to nonlinear stretched sheet with convective condition, Int. J. Heat Mass Tran. 102 (2016) 766–772.
[4] Ji-Huan He, Galal M. Moatimid, Mohamed FE. Amer, EHD stability of a viscid fluid cylinder surrounded by viscous/inviscid gas with fluid-particle mixture in porous media, Results Phys. (2022), 105666.
[5] Ji-Huan He, Galal M. Moatimid, Doaa R. Mostapha, Nonlinear instability of two streaming-superposed magnetic Reiner-Rivlin Fluids by He-Laplace method, J. Electroanal. Chem. 895 (2021), 115388.
[6] A.I. Abderrahmane, S.S. A, et al., Non-Newtonian nanofluid natural convective heat transfer in an inclined Half-annulus porous enclosure using FEM, Alex. Eng. J. 61 (7) (2022) 5441–5453.
[7] M.M. Khader, Ram Prakash Sharma, Evaluating the unsteady MHD micropolar fluid flow past stretching/shirking sheet with heat source and thermal radiation: implementing fourth order predictor–corrector FDM, Math. Comput. Simulat. 181 (2021) 333–350.
[8] Sharma, Ram Prakash, S.R. Mishra, A numerical simulation for the control of radiative heat energy and thermophoretic effects on MHD micropolar fluid with heat source, J. Ocean Eng. Sci. 7 (1) (2022) 92–98.
[9] Sajad Salehi, et al., Hydrothermal analysis of MHD squeezing mixture fluid suspended by hybrid nanoparticles between two parallel plates, Case Stud. Therm. Eng. 21 (2020), 100650.
[10] S.S. Ghadikolaei, et al., MHD boundary layer analysis for micropolar dusty fluid containing Hybrid nanoparticles (Cu-Al2O3) over a porous medium, J. Mol. Liq. 268 (2018) 813–823.
[11] Mohsen Sheikholeslami, Kuppalapalle Vajravelu, Mohammad Mehdi Rashidi, Forced convection heat transfer in a semiannulus under the influence of a variable magnetic field, Int. J. Heat Mass Tran. 92 (2016) 339–348.
[12] N.S. Bondareva, M.A. Sheremet, I. Pop, Magnetic field effect on the unsteady natural convection in a right-angle trapezoidal cavity filled with a nanofluid: Buongiorno's mathematical model, Int. J. Numer. Methods Heat Fluid Flow 25 (2015) 1924–1946.
[13] M. Sheikholeslami, Houman B. Rokni, Numerical modeling of nanofluid natural convection in a semi annulus in existence of Lorentz force, Comput. Methods Appl. Mech. Eng. 317 (2017) 419–430.
[14] Nadezhda S. Bondareva, Mikhail A. Sheremet, Hakan F. Oztop, Nidal Abu-Hamdeh, Heatline visualization of MHD natural convection in an inclined wavy open porous cavity filled with a nanofluid with a local heater, Int. J. Heat Mass Tran. 99 (2016) 872–881.
[15] M. Sheikholeslami, K. Vajravelu, Nanofluid flow and heat transfer in a cavity with variable magnetic field, Appl. Math. Comput. 298 (2017) 272–282.
[16] M.A. Sheremet, H.F. Oztop, I. Pop, K. Al-Salem, MHD free convection in a wavy open porous tall cavity filled with nanofluids under an effect of corner heater, Int. J. Heat Mass Tran. 103 (2016) 955 964.
[17] M. Sheikholeslami, D.D. Ganji, Nanofluid hydrothermal behavior in existence of Lorentz forces considering Joule heating effect, J. Mol. Liq. 224 (2016) 526–537.
[18] M. Sheikholeslami, D.D. Ganji, M.M. Rashidi, Magnetic field effect on unsteady nanofluid flow and heat transfer using Buongiorno model, J. Magn. Magn Mater. 416 (2016) 164–173.
[19] Mohsen Sheikholeslami, Davood Domiri Ganji, Nanofluid flow and heat transfer between parallel plates considering Brownian motion using DTM, Comput. Methods Appl. Mech. Eng. 283 (2015) 651–663.
[20] M. Sheikholeslami, D.D. Ganji, Heat transfer of Cu-water nanofluid flow between parallel plates, Powder Technol. 235 (2013) 873–879.
[21] M. Sheikholeslami, H.R. Ashorynejad, D.D. Ganji, A. Yıldırım, Homotopy perturbation method for three-dimensional problem of condensation film on inclined rotating disk, Sci. Iran. B 19 (3) (2012) 437–442.
[22] M. Sheikholeslami, R. Ellahi, H.R. Ashorynejad, G. Domairry, T. Hayat, Effects of heat transfer in flow of nanofluids over a permeable stretching wall in a porous medium, J. Comput. Theor. Nanosci. 11 (2014) 1–11.
[23] M. Sheikholeslami, D.D. Ganji, H.R. Ashorynejad, Houman B. Rokni, Analytical investigation of Jeffery-Hamel flow with high magnetic field and nano particle by Adomian decomposition method, Appl. Math. Mech. – Engl. Ed. 33 (1) (2012) 1553–1564.
[24] M. Sheikholeslami, D.D. Ganji, H.R. Ashorynejad, Investigation of squeezing unsteady nanofluid flow using ADM, Powder Technol. 239 (2013) 259–265.
[25] M. Sheikholeslami, D.D. Ganji, Magnetohydrodynamic flow in a permeable channel filled with nanofluid, Sci. Iran. B 21 (1) (2014) 203–212.
[26] Mohsen Sheikholeslami, Hamid Reza Ashorynejad, Davood Domairry, Ishak Hashim, Investigation of the laminar viscous flow in a semi-porous channel in the presence of uniform magnetic field using optimal homotopy asymptotic method, Sains Malays. 41 (10) (2012) 1177–1229.
[27] H. Mirgolbabaee, S.T. Ledari, D.D. Ganji, New approach method for solving Duffing-type nonlinear oscillator, Alex. Eng. J. 55 (2016) 1695–1702.
[28] M. Sheikholeslami, M. Nimafar, D. Ganji, Nanofluid heat transfer between two pipes considering Brownian motion using AGM, Alex. Eng. J. 56 (2017) 277–283.
[29] S. Sindhu, B.J. Gireesha, D.D. Ganji, Simulation of Cu: γ− ALOOH/Water in a microchannel heat sink by dint of porous media approach, Case Stud. Therm. Eng. 21 (2020), 100723.
[30] P. Pasha, H. Nabi, D.D. Ganji, Numerical Analysis of Conduction Heat Transfer Flow and the Viscosity of the Fluid Passing through a Flat Channel Using AGM and Flexpde Software, 2022.
[31] Ferdosi, Sima Besharat, Maryam Abasi, Axial buckling of single-walled nanotubes simulated by an atomistic finite element model under different temperatures and boundary conditions, Int. J. Sci. Eng. Appl. 11 (11) (2022) 151–163.
[32] Ali Qasemian, et al., Hydraulic and thermal analysis of automatic transmission fluid in the presence of nano-particles and twisted tape: an experimental and numerical study, J. Cent. S. Univ. 28 (11) (2021) 3404–3417.

[33] Mohammad Bazmi, et al., Nitrogen-doped carbon nanotubes for heat transfer applications: enhancement of conduction and convection properties of water/N-CNT nanofluid, J. Therm. Anal. Calorim. 138 (2019) 69–79.
[34] Chiniforooshan Esfahani, Ilia, A data-driven physics-informed neural network for predicting the viscosity of nanofluids, AIP Adv. 13 (2) (2023), 025206.
[35] P. Sudarsana Reddy, A.J. Chamkha, Soret and Dufour effects on unsteady MHD heat and mass transfer from a permeable stretching sheet with thermophoresis and non-uniform heat generation/absorption, J. Appl. Fluid Mech. 9 (5) (2016) 2443–2455.
[36] P. Sudarsana Reddy, P. Sreedevi, Impact of chemical reaction and double stratification on heat and mass transfer characteristics of nanofluid flow over porous stretching sheet with thermal radiation, Int. J. Ambient Energy 43 (1) (2022) 1626–1636.
[37] P. Sudarsana Reddy, P. Sreedevi, Buongiorno's model nanofluid natural convection inside a square cavity with thermal radiation, Chin. J. Phys. 72 (2021) 327–344.
[38] Patakota Sudarsana Reddy, et al., Heat and mass transfer boundary-layer flow over a vertical cone through porous media filled with a Cu–water and Ag–water nanofluid, Heat Tran. Res. 49 (2018) 2.
[39] P. Sudarsana Reddy, P. Sreedevi, Ali J. Chamkha, Heat and mass transfer flow of a nanofluid over an inclined plate under enhanced boundary conditions with magnetic field and thermal radiation, Heat Tran. Asian Res. 46 (7) (2017) 815–839.
[40] P. Sreedevi, Patakota Sudarsana Reddy, Combined influence of Brownian motion and thermophoresis on Maxwell three-dimensional nanofluid flow over stretching sheet with chemical reaction and thermal radiation, J. Porous Media 23 (2020) 4.
[41] P. Sreedevi, P. Sudarsana Reddy, K.V. Suryanarayana Rao, Effect of magnetic field and radiation on heat transfer analysis of nanofluid inside a square cavity filled with silver nanoparticles: tiwari–Das model, Waves Random Complex Media (2021) 1–19.
[42] P. Sreedevi, P. Sudarsana Reddy, Effect of magnetic field and thermal radiation on natural convection in a square cavity filled with TiO2 nanoparticles using Tiwari-Das nanofluid model, Alex. Eng. J. 61 (2) (2022) 1529–1541.
[43] P. Sreedevi, Patakota Sudarsana Reddy, Williamson Hybrid Nanofluid Flow over Swirling Cylinder with Cattaneo–Christov Heat Flux and Gyrotactic Microorganism, Waves in Random and Complex Media, 2021, pp. 1–28.
[44] P. Sreedevi, P. Sudarsana Reddy, M.A. Sheremet, Impact of homogeneous–heterogeneous reactions on heat and mass transfer flow of Au–Eg and Ag–Eg Maxwell nanofluid past a horizontal stretched cylinder, J. Therm. Anal. Calorim. 141 (2020) 533–546.
[45] Seyyed Masoud Seyyedi, M. Hashemi-Tilehnoee, Mohsen Sharifpur, Impact of fusion temperature on hydrothermal features of flow within an annulus loaded with Nano encapsulated phase change materials (NEPCMs) during natural convection process, Math. Probl Eng. 2021 (2021) 1–14.
[46] M. Hashemi-Tilehnoee, et al., Entropy generation in concentric annuli of 400 kV gas-insulated transmission line, Therm. Sci. Eng. Prog. 19 (2020), 100614.
[47] Alizadeh, Asad, Anas Abid Mattie, Two-Dimensional Simulation To Investigate The Interaction Of Fluid-Structure Inside A Microchannel With Elastic And Rigid Boundary, International Journal of Mechanical and Production Engineering Research and Development (IJMPERD) 9 4 (Aug 2019) 1151–1156, 2019.
[48] Mourad, Abed, et al., The numerical analysis of the melting process in a modified shell-and-tube phase change material heat storage system, Journal of Energy Storage 55 (2022), 100614.